

Double-slit and electromagnetic models to complete quantum mechanics

Jayme De Luca*

Universidade Federal de São Carlos,

Departamento de Física

Rodovia Washington Luis, km 235

Caixa Postal 676, São Carlos, São Paulo 13565-905

(Dated: October 22, 2018)

We analyze a realistic microscopic model for electronic scattering based on the neutral differential delay equations for point charges of the Wheeler-Feynman electrodynamics. We propose a microscopic model according to the electrodynamics of point charges, complex enough to describe the essential physics. Our microscopic model reaches a simple qualitative agreement with the experimental results as regards interference in double-slit scattering and in electronic scattering by crystals. We discuss our model in the light of existing experimental results, including a qualitative disagreement found for the double-slit experiment. We discuss an approximate solution for the neutral differential delay equations of our model using piecewise-defined (discontinuous) velocities for all charges and piecewise-constant-velocities for the scattered charge. Our approximation predicts the De Broglie wavelength as an inverse function of the incoming velocity and in the correct order of magnitude. We explain the scattering by crystals in the light of the same simplified modeling with Einstein-local interactions. We include a discussion of the qualitative properties of the neutral differential delay equations and the boundary-value variational method of electrodynamics to stimulate future experimental tests on the possibility to complete quantum mechanics with electromagnetic models.

Keywords: state-dependent delay; neutral differential delay equation; electrodynamics of point charges; wavelike interference

I. INTRODUCTION

We discuss an attempt to complete quantum mechanics (QM) with an Einstein-local deterministic theory along with an analysis of realistic models for electronic diffraction. We introduce time-dependent interactions with the microscopic electronic trajectories inside the measuring apparatuses as a five-body-problem. We find that a microscopic model with delayed long-range interactions is enough to explain qualitatively the electronic scattering experiments. We analyze the microscopic models with the equations of motion for point charges of the Wheeler-Feynman electrodynamics¹, whose complex qualitative behavior is worth stating clearly. The electromagnetic equations of motion are neutral differential delay equations and have a qualitative behavior quite far from ordinary differential equations (ODE)²⁻⁴. We include a brief discussion of some generic qualitative properties of neutral differential delay equations relevant for the microscopic modeling. As with any modeling, if one starts with a narrow enough setup it is easy to obtain impossibility proofs, and the next step is usually harder, i.e., to define a wider minimum setup. We discuss our models in the light of available experimental work⁵ and a finite variational method for the Wheeler-Feynman electrodynamics⁶.

No single realistic dynamical model based on electrodynamics has been analyzed down to microscopic detail up to now. The existing gap has two causes (i) electrodynamics itself was not a finished theory in the early 20th century; the first equation of motion for a point-charge⁷ appeared in 1938 and a form free of self-interaction¹ only

in 1945 and (ii) the theory of dynamical systems was not out in the early days of point-charge-electrodynamics, neither tools existed to understand the complex dynamics described by differential delay equations. On the other hand there is the popular quantum schism created by failed naive attempts to complete quantum mechanics with a Galilei-invariant mechanics based on ordinary differential equations with globally C^∞ trajectories and instantaneous interactions. Quantum mechanics (QM) was successfully developed as a Machian probabilistic theory, and there are several hints that a dynamics with Newtonian ordinary differential equations is *not* sufficient to complete QM. Even though the simplest quantum operators are pedagogically constructed by analogy with Galilei-invariant mechanics, a classical dynamics with ordinary differential equations is useless either to complete QM *or* to approximate the neutral differential delay equations of motion of point-charge-electrodynamics, as we show here. It is known that the no-go-theorems of Bell type fail for non-instantaneous interactions⁸ even without invoking the generic properties of neutral differential delay equations and variational methods with boundary conditions in the future, as discussed here. Nevertheless, there has been no attempt to complete QM with detailed modeling as regards the double-slit experiment.

This paper is divided as follows: In Section II we discuss existing experimental results on double-slit scattering, including a controlled ballistic experiment that found an unexpected qualitative disagreement⁵ and the later claims⁹ that the double-slit experiment should not display the simple interference based on a single De Broglie wave. We give a simplified model based on electromagnetic trajectories with vanishing far-fields, a model that

explains the qualitative results of interference. In Section III we discuss the equations of motion of point charges of the Wheeler-Feynman electrodynamics and the electromagnetic variational method⁶. In Section III we also work out the details of a model for scattering with each slit represented by a heavy neutral atom, a system with little recoil that is not destroyed upon scattering, unlike a model for bowling. We introduce a simple approximation for the dynamics with (discontinuous) piecewise-defined-velocities and piecewise-constant-velocities for the scattered charge. Our model predicts the qualitative dependence of the De Broglie wavelength on the incoming electronic velocity and calculates the De Broglie wavelength in the correct order of magnitude. In Section IV we put the discussions and conclusion. In appendix A we discuss the qualitative properties of differential delay- and neutral differential delay equations with generic initial conditions. These qualitative properties when included in detailed modeling might offer further possible experimental tests for electromagnetic modeling and the completion of QM. In appendix B we discuss some models for scattering by a periodic crystal. The modeling again reaches a qualitative agreement with the experimental results.

II. ELECTRON SCATTERED BY A DOUBLE-SLIT

Usually, the quantum explanation of double-slit diffraction is contrasted to simple billiard-ball-like-one-body-dynamics, and no microscopic model or time-dependent variables of the apparatus are ever introduced^{10,11}. Let us start by defining this popular no-go modeling of scattering, henceforth called the billiard-ball-model; This model assumes the electron interacts with the slit walls by contact forces only. According to this model, if one closes one slit at a time, an outwardly scattered electron *must* have gone through the open slit without having interacted with the closed slit at all (because interaction is by contact only)¹². Therefore, the statistical pattern at a far screen with both slits open should be the sum of two one-slit patterns, in bold contradiction with the predictions of Schroedinger's equation *and* the experimental results. On the other hand, the popular quantum model of double-slit diffraction is the scalar diffraction for the wave equation, a Schroedinger equation often pedagogically introduced by analogy with billiard-ball dynamics, with a potential vanishing everywhere but at slit boundaries. We stress that even though it is time-proven that the analogy works well from the Galilei-invariant dynamics to abstract quantum operators, using the analogy backwards to construct a dynamical system to complete quantum mechanics is far another problem. The reverse analogy *from* the scalar wave diffraction *to* the billiard-ball dynamics is not granted;

The difficulties with this *reverse analogy* become apparent when we consider the *realistic* quantum mechanical model for a *real electron with spin*, approaching a realistic material slit composed of electrons and protons.

The realistic quantum description is as follows; The incoming electron has a De Broglie distance of influence λ_{DB} , so that its wavefunction overlaps the wavefunctions of the electrons at the material *before* it hits the slit. Because of the exclusion principle, already at a distance λ_{DB} , the electronic spin could flip due to this overlap. Flipping the spin gives the incoming electron an orbital-angular-momentum-kick of the order of \hbar (electronic spin carries an angular momentum of $\sqrt{3}\hbar/2$). This change-by-spin-flip of the orbital-angular-momentum produces diffraction, even *before* the electrons hits any slit. Notice that quantum mechanics with spin suggests that the electron suffers an angular-momentum kick without having to pass by any slit, actually even before going through one of the slits. Therefore, the careful quantum mechanical analysis of diffraction *with spin* suggests a microscopic model with an interaction that can change the orbital angular momentum at-a-distance (rather than a billiard-ball dynamics). If the distance between slits is a and the incoming electron has mass m and velocity v , the largest orbital-angular-momentum about an axis passing by one slit belongs to a trajectory passing by the other slit, i.e., $L = amv$ (higher trajectories simply hit the wall and do not pass to the other side). The largest scattering due to the \hbar angular-momentum-kick of the flipping spin happens when $L = amv \sim \hbar$, i.e.,

$$a = \frac{\hbar}{mv}, \quad (1)$$

which is the familiar slit-separation for significant scattering. In the electromagnetic microscopic modeling the electron interacts with both slits at a distance λ_{DB} before passing through one slit, unlike the interaction by contact of the billiard-ball model. So much to say the confusion generated by the billiard-ball straw-man-model is unacceptable moot.

The first double-slit experiment¹¹ was performed in 1961, obtaining a scattering pattern in qualitative agreement with the quantum predictions. The first ballistic experiment with a single electron in the apparatus at a time¹³ was performed in 1989 by Tonomura et al¹⁰, obtaining a build-up of fringe patterns in qualitative agreement with quantum mechanics and the Huygens interference. It seems that so far no one has claimed quantitative precision beyond order of magnitude for the double-slit experiment. In 1994 an unexpected periodicity was found in a controlled ballistic experiment of double-slit scattering⁵. The anomalous periodicity was later explained⁹ as due to multiple scattering processes, but the quantum mechanical explanation made explicit use of a *realistic* model⁹. The explanation⁹ also made evident the need for a realistic quantum modeling and as a bonus seemed to rule out a precise experimental realization of the popular idealized experiment. This situation

should be contrasted to electronic diffraction in crystals and periodic structures, where Bragg directions can be determined very precisely. For the case of a crystal, the microscopic modeling captures the essential experimental results even with ordinary differential equations, as discussed in appendix B.

In the following we introduce a microscopic model for double-slit-diffraction consisting of the scattered electron in addition to an electron bound to each heavy positive charge at each slit site, which are separated by the slit distance a . Our model uses the Wheeler-Feynman equations of motion of point charges keeping only the far-field interactions. Our simplification stems from four reasons: (i) we disregard the short-range Coulomb interactions that are approximately cancelled by charge neutrality, (ii) we ignore the short-ranged Biot-Savart interactions that are small at low velocities, (iii) we keep the terms that introduce neutral delay in the differential equations, i.e., the far-field-couplings between point charges, which depend on the retarded/advanced accelerations, and (iv) the far-field interactions have the longest range, representing naturally the first physical interaction suffered by the electron when approaching the double-slit and scattering away. We henceforth adopt a unit system where the speed of light is $c = 1$, the electronic charges are $e = -1$ and we label quantities related to each electron with indices $k = 1, 2, 3$. We define trajectories on a Lorentz four-space \mathcal{L}^4 attached to an inertial frame by Einstein synchronization of clocks. A point in \mathcal{L}^4 is defined by a time t and a spatial position \mathbf{x} and we parametrize trajectories by time so that each trajectory is a function $\mathbf{x}_k(t_k) : \mathbb{R} \rightarrow \mathbb{R}^3$. As derived in Section III, the low-velocity equation of motion of charge 1 in the far-field-only approximation is

$$m_1 \frac{d^2}{dt^2} \mathbf{x}_1(t) = \frac{n_{12}^+}{2r_{12}^+} \times [n_{12}^+ \times \frac{d^2}{dt^2} \mathbf{x}_2(t_2^+)] \quad (2)$$

$$+ \frac{n_{12}^-}{2r_{12}^-} \times [n_{12}^- \times \frac{d^2}{dt^2} \mathbf{x}_2(t_2^-)]$$

$$+ \frac{n_{13}^+}{2r_{13}^+} \times [n_{13}^+ \times \frac{d^2}{dt^2} \mathbf{x}_3(t_3^+)]$$

$$+ \frac{n_{13}^-}{2r_{13}^-} \times [n_{13}^- \times \frac{d^2}{dt^2} \mathbf{x}_3(t_3^-)].$$

The equations of motion of the other charges are obtained analogously, by exchanging indices in Eq. (2). In Eq. (2) unit vectors $n_{1k}^\pm \equiv (\mathbf{x}_1(t) - \mathbf{x}_k(t_k^\pm))/|\mathbf{x}_1(t) - \mathbf{x}_k(t_k^\pm)|$ point respectively from the charge's advanced/retarded position $\mathbf{x}_k(t_k)$ to the position of charge 1 at time t . In Eq. (2) the advanced/retarded times are defined by the implicit formulas

$$t_k^\pm = t \pm |\mathbf{x}_k(t_k^\pm) - \mathbf{x}(t)|, \quad (3)$$

and the respective distances in lightcone are defined by

$$r_{1k}^\pm = |\mathbf{x}_k(t_k^\pm) - \mathbf{x}(t)|. \quad (4)$$

Notice that Eq. (2) is a *neutral differential delay equation* with advanced and retarded deviating arguments. In appendix A we review some qualitative properties of delay- and neutral differential delay equations and discuss how, for generic initial data, solutions of delay equations must be defined *piecewise*. Moreover, our approximate equations of motion depend linearly on the accelerations (see Eq. (2)), so that arbitrary piecewise-constant-velocity solutions can be added to any balanced solution of the isolated system of bound charges. In Ref.¹⁵ it is proved that if the bounded motion of two charges has vanishing far-fields, the dynamics of the bounded charges *must* have a sewing chain of velocity discontinuities. This gives rise to a natural forcing period defined by the sewing chains of the bound trajectories, as explained in the following.

As discussed in appendix A, in general a neutral differential delay equation like Eq. (2) has piecewise-defined solutions with discontinuous velocities and accelerations. A discontinuity in the acceleration of particle 1 is propagated in time by Eq. (2), as follows; In Figure 1 we illustrate a point p_0 where the acceleration of charge 3 is discontinuous. The equation of motion for charge 1, Eq. (2), involves the discontinuous past acceleration of charge 3 on the right-hand-side, yielding a discontinuous acceleration for charge 1 at point $f_{31}(1)$. On the equation of motion for charge 3 the discontinuous acceleration of charge 1 at point $f_{31}(1)$ is on the right-hand-side and defines another discontinuity for acceleration 3 at point $f_{31}(2)$. Successively, this produces a sewing chain of acceleration discontinuities at times $f_{31}(k)$, as illustrated in Fig. 1, which define a stroboscopic sampling of each trajectory. The sewing chain involving trajectories 1 and 2 is not illustrated, but it resonates and is part of the dynamics as well. A controlled ballistic experiment on double-slit interference found *two* wavelengths⁵; one near the De Broglie wavelength and another near half the De Broglie wavelength. Our electromagnetic model with state-dependent-delay naturally defines *two* wavelengths by the *four* delayed interactions with the bound electrons, as follows;

The equation of motion (2) and the respective equations for the other charges have oscillatory solutions with decreasing wavelength when the electron approaches the inner gate of scattering. Low-velocity initial conditions approaching the inner gate from the left-hand-side with an exactly horizontal velocity have equal advanced/retarded distances to the bound charges, i.e., $r_{12}^+ \simeq r_{12}^- \simeq r_{13}^+ \simeq r_{13}^- \equiv r$. For example, along trajectory 1 the bouncing times of the advanced interaction are times $f_{31}(1), f_{31}(3), f_{31}(5)$ of Fig. 1, which in the far region are approximately separated by $2r$ and have decreasing time separations until the limiting period a for a perfectly symmetric horizontal velocity hitting the center of the inner gate (which never passes to the other side). In the near region the sewing chain of Fig. 1 starts to resonate also with the sewing chain between trajectories 1 and 2 (not illustrated in Fig. 1), because they share the same frequency. The small vertical velocity

breaks the symmetry in the near region and the state-dependent distances to the bound charges start to differ, defining which slit the scattered charge passes through. The sewing chains for a slightly non-horizontal trajectory 3 excite an effective oscillation with period L superposed to the dynamics of the interacting bound charges.

We henceforth assume that the scattered charge finds a resonant path along which the distances in lightcone to the bound charges are multiples of each other. The sewing chain of interactions with the bound charges excite a period L smaller than the limiting value a of the symmetric centrally horizontal initial condition. In Section III we estimate this resonant wavelength L by the distance of closest approximation between the scattered charge and the atom at the slit it passes through. The calculations assume the bound charges are bound to heavy positive charges sitting at each slit end, so that perturbations imposed by the incoming electron on the bound electrons are passed to the heavy charges at each site, producing smaller perturbations to disturb the scattered electron along its outer scattering path.

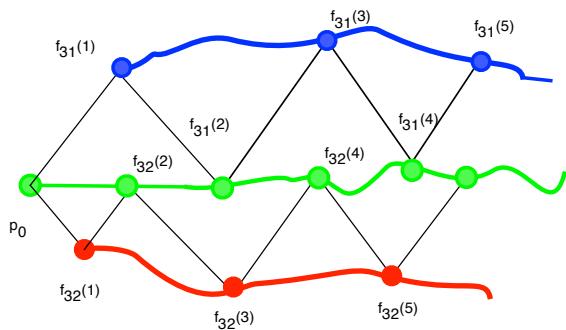


FIG. 1: Illustrated is the trajectory of charge 3 (green) and trajectories of charges 1 (blue) and 2 (red), pictorially displayed along the time direction, even though trajectories 1 and 2 are bounded. The acceleration is discontinuous at point p_0 along trajectory 3, which is connected by the advanced interaction to point $f_{31}(1)$ along trajectory 1, producing a forward sewing chain of breaking points, i.e., points $f_{31}(2)$, $f_{31}(3)$, $f_{31}(4)$ and $f_{31}(5)$. Illustrated is also a sewing chain of discontinuities starting from point p_0 and proceeding in lightcone to trajectory 2, i.e., points $f_{32}(1)$, $f_{32}(2)$, $f_{32}(3)$, $f_{32}(4)$ and $f_{32}(5)$.

The acceleration discontinuities along each bound trajectory oscillate periodically, so that an horizontally traveling third charge interacts with the discontinuity points along each bound orbit simultaneously (by symmetry), so that kicks received from each charge can cancel each other by synchronization. Therefore, the forward scattering direction is a solution by symmetry. Placing the asymptotically scattered constant-velocity in another direction on the right-hand-side of Fig. 2 is tricky because the scattered electron interacts with the discontinuities

along each bound trajectory at *different times*. As discussed in Section III, the scattered velocity must jump to leave the Einstein-local momentum (17) continuous. The options for scattering are the resonant Bragg directions illustrated in Fig. 2, where charge 3 interacts *simultaneously* with the velocity discontinuities along both bound trajectories, so that condition (17) is automatically satisfied with a continuous constant velocity for charge 3. This simple microscopic model is in qualitative agreement with the experimental results on quantum interference. We stress that the sewing chain oscillations illustrated in Fig. 1 are natural for our advanced/retarded equations, *unlike* the case of a model using an instantaneous ODE. For example, the popular model using an ODE with instantaneous short-ranged Coulomb interactions is excluded, as in that respect even an ODE with long-range instantaneous interactions does not display oscillatory sewing chains.

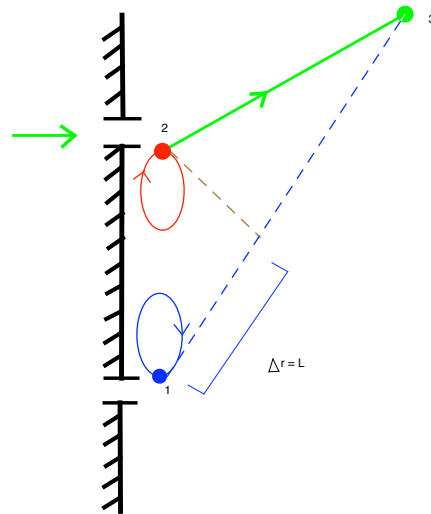


FIG. 2: Illustrated are the bound trajectories of electrons 1 (solid blue) and 2 (solid red) at each material slit and the piecewise-straight-line trajectory of the scattered electron 3 (solid green). Illustrated is the distance from particle 3 to particle 2 (green) and the distance from particle 3 to particle 1 (blue). The different distances from electron 3 to the bound trajectories define a different delay for each interaction, which resonates when this difference is equal to the period L .

Our simplified model explains the qualitative properties of quantum double-slit scattering; namely (i) Existence of favored lateral directions of scattering controlled by Bragg interference, which is due to the state-dependent delay, (ii) Existence of a forward direction of scattering by the double-slit system, and (iii) Scattering with one slit closed at a time defines only a forward scattering peak while scattering with both slits open displays interference. The interference is due to the long-range nature of the forces and is present in any model with interaction-at-a-distance. The specific form of our interference turned out to be wavelike *because* we used the electrodynamics of point-charges, which inher-

ited state-dependent-delay from Maxwell's wave theory. Other models with long-range interactions should display interference as well, but perhaps not precisely wave-like. In the next section we discuss a far-field model with piecewise-constant-velocities that predicts the inverse dependence of the De Broglie wavelength on the incoming particle velocity and yields a value in the correct order of magnitude.

III. PIECEWISE-DEFINED-SOLUTIONS AND FAR-FIELD-MODEL

In the Wheeler-Feynman electrodynamics one does not solve differential equations for the electromagnetic fields, but rather the trajectories are the critical points (minimizers) of a variational method with mixed-type boundaries⁶. The electromagnetic fields are simply the coupling terms to the other particle's trajectories as defined by the Euler-Lagrange equations of the variational method. Rigorously speaking, these Euler-Lagrange-coupling-fields are defined only *on* the trajectories, even though given by the exact same usual formulas of Maxwell's electrodynamics⁶. Our model uses the equations of motion of point charges keeping only the far-field interactions. We disregard the short-range Coulomb interactions that are approximately cancelled by charge neutrality and ignore the short-range Biot-Savart interactions that are small at low velocities. In a unit system where $c = e = 1$, the low-velocity Wheeler-Feynman equations of motion can be expressed in the familiar form⁶

$$m_k \frac{d^2}{dt^2} \mathbf{x}_k(t) = -\mathbf{E}(\mathbf{x}_k, t) - \mathbf{v}_k \times \mathbf{B}(\mathbf{x}_k, t), \quad (5)$$

where $\mathbf{v}_k \equiv d\mathbf{x}_k(t)/dt$. The electric far-field-coupling-term for each point-charge in the Wheeler-Feynman electrodynamics is given by a semi-sum of advanced and retarded fields¹,

$$\mathbf{E}(\mathbf{x}, t) = \frac{1}{2} \mathbf{E}^+(\mathbf{x}, t) + \frac{1}{2} \mathbf{E}^-(\mathbf{x}, t), \quad (6)$$

while the far-magnetic field is given by

$$\mathbf{B}(\mathbf{x}, t) = \frac{1}{2} \mathbf{n}_+ \times \mathbf{E}^+(\mathbf{x}, t) - \frac{1}{2} \mathbf{n}_- \times \mathbf{E}^-(\mathbf{x}, t), \quad (7)$$

where unit vectors $\mathbf{n}_k^\pm \equiv (\mathbf{x} - \mathbf{x}_k(t_k^\pm))/|\mathbf{x} - \mathbf{x}_k(t_k^\pm)|$ point respectively from the charge's advanced/retarded position $\mathbf{x}_k(t_k)$ to point \mathbf{x} at time t (see Chapter 14 of¹⁴). The far-electric and far-magnetic field of each charge k are defined piecewise by the Liénard-Wiechert formulas¹⁴

$$\mathbf{E}_k^\pm(\mathbf{x}, t) = \frac{-\mathbf{n}_k^\pm}{r_k^\pm} \times \frac{[(\mathbf{n}_k^\pm \pm \mathbf{v}_k^\pm) \times \mathbf{a}_k^\pm]}{(1 \pm \mathbf{n}_k^\pm \cdot \mathbf{v}_k^\pm)^3}, \quad (8)$$

and

$$\mathbf{B}_k^\pm(\mathbf{x}, t) = \mp \frac{\mathbf{n}_k^\pm}{r_k^\pm} \times \left[\frac{\mathbf{a}_k^\pm}{(1 \pm \mathbf{n}_k^\pm \cdot \mathbf{v}_k^\pm)^2} \mp \frac{(\mathbf{n}_k^\pm \cdot \mathbf{a}_k^\pm) \mathbf{v}_k^\pm}{(1 \pm \mathbf{n}_k^\pm \cdot \mathbf{v}_k^\pm)^3} \right], \quad (9)$$

where the advanced/retarded times are functions of t and \mathbf{x} given by

$$t_k^\pm = t \pm |\mathbf{x}_k(t_k^\pm) - \mathbf{x}|, \quad (10)$$

and the distances in lightcone are functions of t and \mathbf{x} defined as

$$r_k^\pm = |\mathbf{x}_k(t_k^\pm) - \mathbf{x}|, \quad (11)$$

where t_k is defined by Eq. (10). In Eqs. (8) and (9) $\mathbf{v}_k^\pm \equiv d\mathbf{x}_k/dt_k|_{t_k^\pm}$ and $\mathbf{a}_k^\pm \equiv d^2\mathbf{x}_k/dt_k^2|_{t_k^\pm}$ are respectively the charge's velocity and acceleration at the advanced/retarded time t_k^\pm . It is possible to show that the derivative of the advanced/retarded time respect to t is given by

$$\frac{dt_k}{dt} = \frac{1}{(1 \pm \mathbf{n}_k^\pm \cdot \mathbf{v}_k^\pm)}, \quad (12)$$

using Eq. (10) and the chain rule. Using Eqs. (9) and (10) with the chain rule we can re-write the far-magnetic field as

$$\mathbf{B}_k^\pm(\mathbf{x}, t) = \mp \frac{\mathbf{n}_k^\pm}{r_k^\pm} \times \frac{\partial^2}{\partial t^2} \mathbf{x}_k(t_k^\pm), \quad (13)$$

where the partial derivative indicates that Eq. (10) is to be used with \mathbf{x} as a fixed argument. Finally, the far-electric field is given by

$$\mathbf{E}_k^\pm(\mathbf{x}, t) = \pm \mathbf{n}_k^\pm \times \mathbf{B}_k^\pm(\mathbf{x}, t). \quad (14)$$

The far-field at each charge is the semi-sum of the advanced and the retarded fields (13) and (14) of the other two charges. For example, the low-velocity equation of motion of charge 1, (Eq. (5) with $k = 1$), is a simple-looking neutral differential delay equation

$$\begin{aligned} m_1 \frac{d^2}{dt^2} \mathbf{x}_1(t) = & \frac{(n_{12}^+ + \mathbf{v}_1^+)}{2r_{12}^+} \times [n_{12}^+ \times \frac{\partial^2}{\partial t^2} \mathbf{x}_2(t_2^+)] \quad (15) \\ & + \frac{(n_{12}^- - \mathbf{v}_1^-)}{2r_{12}^-} \times [n_{12}^- \times \frac{\partial^2}{\partial t^2} \mathbf{x}_2(t_2^-)] \\ & + \frac{(n_{13}^+ + \mathbf{v}_1^+)}{2r_{13}^+} \times [n_{13}^+ \times \frac{\partial^2}{\partial t^2} \mathbf{x}_3(t_3^+)] \\ & + \frac{(n_{13}^- - \mathbf{v}_1^-)}{2r_{13}^-} \times [n_{13}^- \times \frac{\partial^2}{\partial t^2} \mathbf{x}_3(t_3^-)], \end{aligned}$$

where the $\mathbf{x}_k(t_k^\pm)$ for $k = 2, 3$ are implicit functions of time t by Eqs. (10) with $\mathbf{x} \equiv \mathbf{x}_1(t)$. The equations of motion for the other (negative) charges are obtained by exchanging indices in Eq. (15), and Eq. (2) is the low-velocity-limit obtained by dropping the velocity terms of the right-hand-side of Eq. (15).

The fields of the heavy positive charges are essential to cancel the short-range Coulomb interaction and might participate to create vanishing far fields¹⁶. In turn, the motion of the bound electrons, henceforth assumed periodic, is essentially responsible to create a vanishing far-field that leaves the scattered electron undisturbed at large distances. For this, velocity discontinuities of the bound electrons are absolutely needed, as follows; As shown in¹⁵, if a bounded motion of two charges produces a net far-field that vanishes almost everywhere, then their trajectories *must* have discontinuous velocities on sewing chains¹⁵. This is the physical need for discontinuous velocities. Vice-versa, the scattered electron can go out in a motion with piecewise-constant-velocity that produces no far-fields (because of Eqs. (8) and (9)), leaving the bound charges undisturbed. An approximation capturing the essentials of this five-body-dynamics is by orbits with discontinuous velocities¹⁵ of the electromagnetic variational method⁶. In the following we approximate the trajectory of scattered charge 3 by two segments with piecewise-constant-velocity, having a single point where velocity 3 is discontinuous.

An orbit with a discontinuous velocity can be a minimizer of the variational method only if some other velocity is discontinuous in the past/future lightcone, in a way that conserves an Einstein-local momentum¹⁵. For these minimizers, the Wheeler-Feynman equations of motion hold *piecewise*, and at velocity discontinuity points an additional condition for an extremum is the continuity of an Einstein-local-spin-like-four-momentum¹⁵ (γ_i, P_i) with

$$\gamma_i \equiv \frac{m_i c}{\sqrt{c^2 - \mathbf{v}_i^2}} - \sum_{j \neq i} \left[\frac{\left(\frac{e^2}{2c}\right)}{r_{ij-}(c - \mathbf{n}_{ij-} \cdot \mathbf{v}_{j-})} + \frac{\left(\frac{e^2}{2c}\right)}{r_{ij+}(c + \mathbf{n}_{ij+} \cdot \mathbf{v}_{j+})} \right], \quad (16)$$

and vector component

$$P_i \equiv \frac{m_i c \mathbf{v}_i}{\sqrt{c^2 - \mathbf{v}_i^2}} - \sum_{j \neq i} \left[\frac{\left(\frac{e^2}{2c}\right) \mathbf{v}_{j-}}{r_{ij-}(c - \mathbf{n}_{ij-} \cdot \mathbf{v}_{j-})} + \frac{\left(\frac{e^2}{2c}\right) \mathbf{v}_{j+}}{r_{ij+}(c + \mathbf{n}_{ij+} \cdot \mathbf{v}_{j+})} \right], \quad (17)$$

which must be *continuous* at each velocity discontinuity point of *each* continuous trajectory, despite the discontinuous velocities on both trajectories¹⁵. Equations (17) and (16) are written in a unit system where the speed of light is c and the electronic charge is e , in order to make dimensional dependences explicit. In the following we use discontinuous trajectories as an intuitive approximation tool to estimate the dynamics without having to solve the detailed state-dependent neutral differential delay equations.

In order to introduce a single discontinuity for the scattered velocity, our simplification further assumes that at

its velocity-discontinuity-point charge 3 sees the single discontinuity of velocity 1 at a distance L and the discontinuity of velocity 2 also in lightcone at a larger distance nL . The velocity discontinuities along the bound orbits must either see each other in lightcone (which requires a resonance), or we must introduce a larger number of velocity discontinuities. After the collision, the bound electron collides with the heavy positive charge, avoiding the destruction of the scattering system by moderating the size of velocity discontinuities. The remaining excited oscillations have a subsequent influence on the out-scattered charge. In this situation we can produce the following estimate for the De Broglie wavelength; We use Eq. (17) to estimate the distance of closest approximation L at the discontinuity point where charge 3 collides with the bound charge and its vertical velocity 3 jumps from zero to a value of the order of $|\mathbf{v}_3|$. The vertical component of Eq. (17) yields the estimate

$$m_3 |\mathbf{v}_3| \simeq \frac{\frac{e^2}{c} |\mathbf{v}_{1-}|}{L(c - \mathbf{n}_{31-} \cdot \mathbf{v}_{1-})}, \quad (18)$$

where we have assumed $(c - \mathbf{n}_{31-} \cdot \mathbf{v}_{1-}) \simeq (c + \mathbf{n}_{31+} \cdot \mathbf{v}_{1+})$ and $|\mathbf{v}_{1-}| \simeq |\mathbf{v}_{1+}|$. The collision is not necessarily a small perturbation on the bound electron's dynamics, and the denominator on the right-hand-side of Eq. (18) can be large, as for example when \mathbf{v}_{1-} performs fast solenoidal ping-pong motions¹⁶. Notice that Eq. (18) yields the experimentally tested De Broglie length inversely proportional to the incoming velocity. The bound electron subsequently collides with the heavy positive charge at the slit end (a proton of mass m_p), sharing the momentum recoil and healing most of its velocity discontinuity. Otherwise the scattered electron destroys the scattering system and we are studying a bowling problem. We have at hand a *five-body-problem* with *ten* state-dependent delays of neutral type. Our approximation introduces a single velocity discontinuity along the scattered trajectory, which must be compensated by a velocity discontinuity in lightcone along the orbit of the bound electron. Velocity discontinuities balance in lightcone by producing continuous momenta (Eqs. (17) and (16)) at (the) breaking point(s) along the protonic trajectory and at (the) breaking point(s) along the trajectory of the bound electron, i.e.,

$$\frac{m_p c}{\sqrt{c^2 - \mathbf{v}_p^2}} - \frac{e^2/c}{r(c - \mathbf{n}_{pe-} \cdot \mathbf{v}_{1-})} \simeq 0, \quad (19)$$

$$\frac{m_e c}{\sqrt{c^2 - \mathbf{v}_{1-}^2}} - \frac{e^2/c}{r(c - \mathbf{n}_{ep-} \cdot \mathbf{v}_p)} \simeq 0, \quad (20)$$

where r is the distance in lightcone at the subsequent collision and \mathbf{v}_p is the (assumed small) protonic velocity, so that we ignore denominators depending on \mathbf{v}_p in Eqs. (19). We further assume $(c - \mathbf{n}_{pe-} \cdot \mathbf{v}_{1-}) \simeq (c + \mathbf{n}_{pe+} \cdot \mathbf{v}_{1+}) \simeq (c - \mathbf{n}_{31-} \cdot \mathbf{v}_{1-}) \simeq c - |\mathbf{v}_{1-}|$, so that eliminating

r from Eqs. (19) yields

$$\frac{c}{(c - \mathbf{n}_{31-} \cdot \mathbf{v}_{1-})} \simeq \left(\frac{\sqrt{2}m_p}{m_e}\right)^{2/3}, \quad (21)$$

and the De Broglie length $\lambda_{DB} = L$ defined by Eq. (18) is

$$\lambda_{DB} = \left(\frac{\sqrt{2}m_p}{m_e}\right)^{2/3} \left(\frac{e^2}{c}\right) \frac{1}{m_3|\mathbf{v}_3|}. \quad (22)$$

Formula (22) yields a length four times smaller than the popular double-slit formula, a rough estimate relying on an approximate solution with discontinuous velocities of variational electrodynamics. In our five-body model, the electron interacts with a disturbance it has created, much like the experiment of Ref.¹⁷

Apart from a proportionality factor, the dependence $\hbar \propto (m_p/m_e)^{2/3}$ is singled out as the only power-law consistent with the hydrogenoid spectroscopic formula, as follows; The spectroscopic frequency of the hydrogen spectrum for the $n_1 \rightarrow n_2$ transition is

$$w_{12} = \frac{m_e e^4}{2\hbar^3} \left(\frac{1}{n_1^2} - \frac{1}{n_2^2}\right). \quad (23)$$

If the protonic mass is multiplied by two, as for a deuterium atom, our power 2/3 law predicts a four-times-larger \hbar^3 , so that the spectroscopic frequency (23) scales to another line of the hydrogen spectrum, i.e., the frequency of the $2n_1 \rightarrow 2n_2$ transition. Together with the estimates of the spectroscopic lines¹⁶, estimate (22) of the De Broglie length suggests that Wheeler-Feynman electrodynamics generalized to discontinuous velocities can offer an alternative to complete quantum mechanics. The derivation of a fundamental formula like Eq. (22) is foreign to the Machian mentality of quantum mechanics; Notice that even though Eq. (22) was derived using a hydrogen atom at each slit end, another model using a heavier atom with n electrons and a proportionally larger nuclear mass nm_p yields the same estimate because there are n electrons to share the recoil in Eqs. (19). A model using a large number of atoms along the inner gate of length a would also lead to the same estimate, so that formula (22) is somewhat "universal".

IV. DISCUSSIONS AND CONCLUSION

The danger of replacing the Wheeler-Feynman equations of motion¹ by a Coulombian ODE, besides lack of Poincaré invariance, are that these are only part of the conditions for a minimizer of the boundary-value variational method with boundaries in past and future¹⁵. As for the fact that these two-body equations of motion *seem* to reduce "formally" to a Coulombian ODE at low velocities and large separations, the qualitative theory of

appendix A teaches us that reduction to an ODE with C^∞ trajectories is not granted with a neutral differential delay equation¹⁵. From the perspective of the variational method with boundaries in past and future^{6,15}, the set of boundary conditions leading to a many-body dynamics with C^∞ trajectories is probably a set of measure zero. As discussed in appendices A and B, this is certainly not the most general set of initial conditions and it is unlikely that initial conditions leading to C^∞ smooth motions with no velocity/acceleration discontinuities are ever going to be met in experiments. More likely a larger class of initial conditions may lead to solutions where discontinuities do not explode asymptotically and stay bounded by laboratory walls (i.e., respect the constraints of the microscopic model). The fact that the electromagnetic variational method has boundaries in past and future^{6,15} is a warning for Bell-type proofs not to assume reduction to an ODE, at variance with the two-point-boundary-value problem of Hamilton's principle of instantaneous Newtonian mechanics. Even reduction to piecewise C^2 orbits is an extra hypothesis that narrows down the qualitative possibilities of the boundary value variational method of electrodynamics¹⁵. We hope to enrich the attempts to complete QM and to prevent/enlighten attempts at impossibility proofs based on "microscopic modeling with trajectories".

We have started on detailed modeling motivated by the subsequent works⁹ that tried to explain the unexpected experimental result⁵. In the light of a detailed model with an interaction-at-a-distance rather than by contact, the contradictions of the billiard-ball-model disappear. Unfortunately, the subsequent explanations⁹ of the experimental disagreement⁵ seem to suggest that the double-slit experiment does not have a simple quantitative/qualitative precision, or it might have provided a testbed for microscopic modeling. Notice that the Wheeler-Feynman electrodynamics with neutral differential delay equations is an Einstein-local theory of interactions; The velocity discontinuities along sewing chains involve only Einstein-local-two-body-events connected by a lightcone⁶, much like "Einstein-local-quantum-jumps". The agreement of our far-field-and-piecewise-constant-velocities-model with the De Broglie wavelength is a test for the use of minimizers with discontinuous velocities to approximate the solutions of the electromagnetic variational method⁶. In fact, the success of our simple model of Section III to complete quantum mechanics suggests that the electromagnetic variational method⁶ is a physically sensible completion for the electrodynamics of point-charges.

Several (if not all) of the popular failures to complete quantum mechanics with electrodynamics stem from the fact that electrodynamics of point-charges with C^∞ trajectories is an incomplete theory¹⁵. The popular reverse-analogy with quantum mechanics suggested in the 1930's an electrodynamics formally analogous to the instantaneous Hamiltonian dynamics, a straw-man to generate impossibility proofs and conundrums. The subse-

quent search for a quantization procedure starting from a Hamiltonian lead to the famous stall of the Wheeler-Feynman program²⁶ in the days before the no-interaction theorem²². The no-interaction theorem²² of 1963 was probably the first serious obstacle for the reverse-analogy approach in the days before the dynamical systems theory.

The electromagnetic variational method⁶ with boundary data yielding globally C^2 orbits contains the reverse-analogy electrodynamics as the poor cousin. Ignoring the dynamical systems theory of appendix A, several *formal* embeddings of electrodynamics into a renormalized Hamiltonian dynamics used expansions of delayed arguments about non-generic C^∞ trajectories, expansions that are meaningless along orbits with discontinuous velocities. Besides expansion of delayed arguments, Dirac's derivation of the self-force⁷ used Poynting's theorem, which holds only for globally C^2 orbits¹⁵. The abundance of runaways of the Dirac electrodynamics of point charges again suggests that physics lies with the discontinuous-velocity-solutions of the boundary-value-variational-electrodynamics⁶.

The leading motivation to construct the boundary-value-variational-method⁶ was to pave the way to study the electromagnetic-two-body-problem *numerically*. Additional tests for the variational electrodynamics with discontinuous velocities would be a microscopic model for Rutherford scattering. Also a detailed model for Compton scattering on wax²⁸ should include many electrons and a heavy nucleus, as discussed below Eq. (23) of Section III. Further understanding on this neutrally-delayed dynamics should come after the development of a robust numerical integrator. A variational integrator shall be published elsewhere along with some numerical experiments.

V. ACKNOWLEDGEMENTS

We acknowledge partial support from FAPEP and CNPQ. We thank an anonymous referee from FAPESP that, in the year 2006, refused an unrelated project of ours on grounds that some day we might try to explain diffraction using electrodynamics. The author is solely responsible for opinions or whatever errors may yet linger in the manuscript. We acknowledge interesting discussions at an early stage with Karl Hess, Michael Mackey and Paulo Farinas. We thank Tony Humphries and Savio Rodrigues for a numerical integrator that first faced us with discontinuous accelerations. We thank Marcel Novaes, Coraci Malta and Karl Hess for reading the later version of the manuscript.

VI. FIGURE CAPTIONS

Figure 1; Illustrated is the trajectory of charge 3 (green) and trajectories of charges 1 (blue) and 2 (red), pictorially displayed along the time direction, even though trajectories 1 and 2 are bounded. The acceleration is discontinuous at point p_0 along trajectory 3, which is connected by the advanced interaction to point $f_{31}(1)$ along trajectory 1, producing a forward sewing chain of breaking points, i.e., points $f_{31}(2)$, $f_{31}(3)$, $f_{31}(4)$ and $f_{31}(5)$. Illustrated is also a sewing chain of discontinuities starting from point p_0 and proceeding in lightcone to trajectory 2, i.e., points $f_{32}(1)$, $f_{32}(2)$, $f_{32}(3)$, $f_{32}(4)$ and $f_{32}(5)$.

Figure 2; Illustrated are the bound trajectories of electrons 1 (solid blue) and 2 (solid red) at each material slit and the piecewise-straight-line trajectory of the scattered electron 3 (solid green). Illustrated is the distance from particle 3 to particle 2 (green) and the distance from particle 3 to particle 1 (blue). The different distances from electron 3 to the bound trajectories define a different delay for each interaction, which resonates when this difference is equal to the period L .

Figure 3; Illustrated in red is a C^1 initial condition for a scalar delay-differential-equation and the orbit (in black) after $t = 0$. The derivative from the left at the initial time $t = 0$ is given by the history and in general differs from the derivative from the right along the continuous orbit. At $t = 1$ the solution is already C^1 .

Figure 4; Illustrated in red is a C^1 initial condition for a scalar neutral-delay-differential-equation and the orbit (in black) after $t = 0$. The derivative from the left at $t = 0$ is given by the history and in general differs from the derivative from the right along the continuous orbit. At $t = 1$ the solution still has a kink in the derivative, a discontinuity that generically propagates to the breaking point at $t = 2$ and to all successive breaking points.

VII. APPENDIX A: DELAY- AND NEUTRAL-DIFFERENTIAL DELAY EQUATIONS

Since the electromagnetic equations of motion are state-dependent neutral differential delay equations⁶, in the following we discuss briefly the qualitative properties of delay- and neutral differential delay equations²⁻⁴. We start with constant delay to simplify the exposition. A delay equation for a scalar function is defined as

$$\frac{dy}{dt} = F(y(t), y(t-1)), \quad (24)$$

where $F(a, b)$ is usually a given C^∞ function. The right-hand-side of Eq. (24) depends of the present value $y(t)$ and the past value $y(t-1)$, so that to construct a unique

solution to Eq. (24) starting from $t = 0$ one needs to provide $y(t)$ on the entire segment $t \in (-1, 0)$. In Figure 3 a typical C^1 initial condition is illustrated in red while the ensuing continuous trajectory is illustrated in black. Notice in Fig. 3 that the derivative from the left at $t = 0$ is given by the derivative of the arbitrary history (red) while the derivative from the right at $t = 0$ is $F(y(0), y(-1))$. The necessary initial history segment and a discontinuous derivative at the starting point are not seen in the simpler integration of ordinary differential equations. For an ODE the initial value $y(0)$ determines a unique solution up to a maximum time t_F where $F(y)$ ceases to be Lipschitz-continuous. In solving Eq. (24) with an arbitrary C^1 history there is a discontinuous derivative at the starting point, so that one can not impose Eq. (24) at $t = 0$. Assuming the initial condition is such that a solution exists, things are no so bad because Eq. (24) holds onwards, and moreover the kink at $t = 0$ smooths out, as follows. At $t = 1$ when Eq. (24) first accesses $t = 0$ as a past point, the left- and right-derivatives predicted by Eq. (24) are equal precisely because the trajectory is continuous, so that the solution $y(t)$ is C^1 at $t = 1$. Successively, when the smoothed point $t = 1$ is first accessed by Eq. (24) at $t = 2$ the derivative of Eq. (24) exists, so that the solution became C^2 , and so on, acquiring more derivatives at successive points where t is a multiple of the delay, henceforth called "breaking points"²⁻⁴. It is usual in solving delay equations numerically² to restrict to derivatives from the left and derivatives from the right at breaking points. Last, for equations with state-dependent delay the breaking points depend on the solution, instead of being simple equally-spaced multiples of the constant delay. If the deviating argument is a monotonically increasing function of time, the above smoothing is also the generic behavior expected for state-dependent-delay.

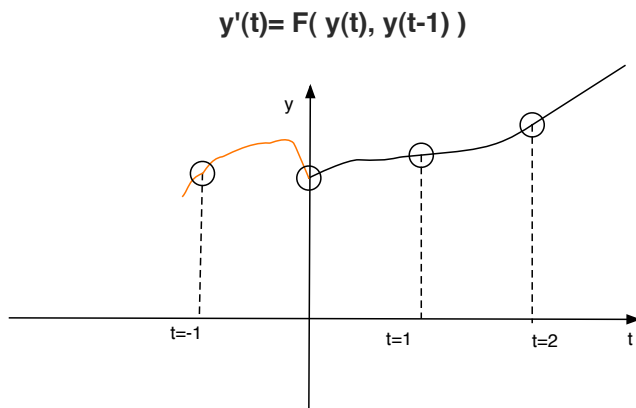


FIG. 3: Illustrated in red is a C^1 initial condition for a scalar delay-differential-equation and the orbit (in black) after $t = 0$. The derivative from the left at the initial time $t = 0$ is given by the history and in general differs from the derivative from the right along the continuous orbit. At $t = 1$ the solution is already C^1 .

The integration of a *neutral differential delay equation* for a scalar function with generic initial data is different, as follows; We start again with constant delay to simplify the exposition²⁻⁴. A neutral differential delay equation for a scalar function is defined as

$$\frac{dy}{dt} = G(y(t), y(t-1), \dot{y}(t-1)), \quad (25)$$

where $G(a, b, c)$ is a given C^∞ function. The right-hand-side of Eq. (25) depends on the present value $y(t)$, on the past value $y(t-1)$ and on the past value of the derivative $\dot{y}(t-1)$. A differential delay equation is said to be a neutral differential delay equation when the derivative depends on a past value of the derivative itself, as seen in Eq. (25). To construct a unique solution to Eq. (25) starting from $t = 0$ again we need to provide $y(t)$ for $t \in (-1, 0)$ and moreover a C^1 initial history is needed because Eq. (25) uses the past derivative. As we already know, the constructed derivative is discontinuous, as illustrated in Fig. 4 for a typical C^1 initial history (red). In Fig. 4 the ensuing continuous trajectory is illustrated in black. Notice that when point $t = 0$ is first accessed at $t = 1$ along the continuous solution, the derivatives predicted by Eq. (25) from the left and from right of $t = 1$ are different. We must therefore restrict to left and right derivatives at breaking points, so that solutions are defined only between breaking points. At $t = 2$ when point $t = 1$ is first accessed from the right along the continuous solution, the derivative discontinuity is still seen by $G(y(t), y(t-1), \dot{y}(t-1))$, unlike the case of Eq. (24). In general for a neutral differential delay equation the derivative could stay discontinuous at all breaking points²⁻⁴. Surprisingly, having derivatives undefined on a set of measure zero is irrelevant for a variational method that involves an integral over the velocities⁶, but nevertheless an important qualitative difference. So much for continuous solutions of one-component delay equations like Eqs. (24) and (25).

Again, the difference to neutral differential delay equations with state-dependent delay is that breaking points depend on the solution, instead of being simple equally-spaced multiples of the constant delay. In the general case of neutral differential delay equation, there is the extra complexity of solution termination² when the deviating argument are *not* monotonically increasing functions of time. Otherwise continuation is possible with discontinuous derivatives. In the case of electrodynamics, deviating arguments are always increasing⁶, so termination does not happen and continuation is always possible. In order to make the forward continuation well-posed, one needs a rule to calculate each velocity discontinuity, like for example our Einstein-local momentum continuity Eqs. (17) and (16) of Section III. The Wheeler-Feynman equations for the two-body problem are expressible in the form (25) using a 12-component vector $y(t)$, particle positions taking up 6 components while particle velocities take up the other 6 components. The smoothing properties of solutions of many-component

$$\mathbf{y}'(t) = \mathbf{G}(\mathbf{y}(t), \mathbf{y}(t-1), \mathbf{y}'(t-1))$$

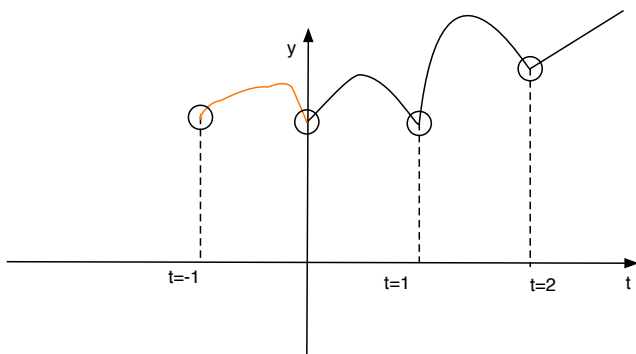


FIG. 4: Illustrated in red is a C^1 initial condition for a scalar neutral differential delay equation and the orbit (in black) after $t = 0$. The derivative from the left at $t = 0$ is given by the history and in general differs from the derivative from the right along the continuous orbit. At $t = 1$ the solution still has a kink in the derivative, which in general does not vanish and propagates to the next breaking point at $t = 2$ and to all successive breaking points.

differential delay equations are similar to the neutral differential delay case²⁹. For example, the 18-component retarded-only two-body equations of motion of Dirac's electrodynamics⁷ can have solutions along which some components are continuous (e.g. the positions) while the velocities and accelerations are discontinuous at *all* the subsequent breaking points²⁹.

VIII. APPENDIX B: ELECTRON (OR NEUTRON) SCATTERED BY A CRYSTAL

We give an example that illustrates how a wave theory is not needed for the explanation of electronic diffraction by crystals¹⁸, a simple but not so popular result. Unlike double-slit scattering, the interference found in crystalline scattering can be explained by a billiard-ball Hamiltonian model with instantaneous contact forces, even though certainly not a fundamental explanation. Next and in sake of an explanation compatible with the theory of relativity, we discuss modeling crystalline scattering with neutral differential delay equations, analogously to Section II. The simple model of Section II uses very little of electrodynamics and is based on a simple Einstein-local continuity of momentum. Any Einstein-local theory for nuclear interactions could be used with the same model to explain neutron diffraction¹⁹. Several early works have explained diffraction by a crystal using the old quantum mechanics, which is based in Hamiltonian mechanics^{20,21}.

Our Hamiltonian model assumes that the incoming electron interacts with the bound electrons of a generic

crystal through an instantaneous Hamiltonian interaction with a periodic potential. We consider a generic Hamiltonian ordinary differential equation (ODE) with a periodic potential, i.e.,

$$H = \frac{1}{2}|\mathbf{p}|^2 + \epsilon \sum_{\mathbf{G}} V_{\mathbf{G}} \exp(i\mathbf{G} \cdot \mathbf{x}), \quad (26)$$

where summation is over reciprocal vectors of any generic periodic lattice. We use complex notation in Eq. (26), with the condition that the potential is real, i.e., $V_{-\mathbf{G}} = V_{\mathbf{G}}^*$, and ϵ is included because we assume the potential is small. The dynamics of Hamiltonian (26) is not integrable in general but it can nevertheless be simplified with a canonical transformation designed to remove the potential, i.e., to transform the Hamiltonian into the free particle Hamiltonian to lowest order in ϵ . The conditions for this simplification are as follows; We choose a simplifying quasi-identity canonical transformation²⁴, with generating function depending on the old coordinate \mathbf{x} and new momentum \mathbf{P}

$$F(\mathbf{x}, \mathbf{P}) = \mathbf{x} \cdot \mathbf{P} + \epsilon \sum_{\mathbf{G}} F_{\mathbf{G}} \exp(i\mathbf{G} \cdot \mathbf{x}), \quad (27)$$

where the $F_{\mathbf{G}}$ are so far arbitrary, respecting only the reality condition $F_{-\mathbf{G}} = F_{\mathbf{G}}^*$. The old momentum \mathbf{p} is related to the new \mathbf{P} by

$$\mathbf{p} = \frac{\partial F}{\partial \mathbf{x}} = \mathbf{P} + \epsilon \sum_{\mathbf{G}} i\mathbf{G} F_{\mathbf{G}} \exp(i\mathbf{G} \cdot \mathbf{x}). \quad (28)$$

Substitution of \mathbf{p} given by Eq. (28) into Eq. (26) yields, up to the first order in ϵ , that the new Hamiltonian is

$$\tilde{H} = \frac{1}{2}|\mathbf{P}|^2 + \epsilon \sum_{\mathbf{G}} [V_{\mathbf{G}} + i(\mathbf{G} \cdot \mathbf{P})F_{\mathbf{G}}] \exp(i\mathbf{G} \cdot \mathbf{x}) + O(\epsilon^2). \quad (29)$$

Hamiltonian \tilde{H} of Eq. (29) is still expressed in terms of the old coordinate \mathbf{x} and the substitution $\mathbf{x} = \mathbf{X}$ into Eq. (29) is only an $O(\epsilon^2)$ mistake. We want to fix the coefficients $F_{\mathbf{G}}$ to vanish the first-order terms of \tilde{H} as given by Eq. (29), so that the new momentum \mathbf{P} is a constant of motion. First let us choose this constant vector \mathbf{P} such that $\mathbf{G} \cdot \mathbf{P} \neq 0$ for all vectors of the reciprocal lattice, a procedure yielding the $F_{\mathbf{G}}$ by

$$F_{\mathbf{G}} = \frac{-iV_{\mathbf{G}}}{\mathbf{G} \cdot \mathbf{P}}, \quad (30)$$

and the new Hamiltonian, Eq. (29), becomes the free-particle Hamiltonian up to the first order in ϵ , i.e.;

$$\tilde{H} = \frac{1}{2}|\mathbf{P}|^2 + O(\epsilon^2), \quad (31)$$

having straight-line trajectories up to times of order $1/\epsilon^2$ and a constant \mathbf{P} as already mentioned. The conclusion is that the trajectory is an approximate straight-line for

most initial conditions, i.e., if $\mathbf{G} \cdot \mathbf{P} \neq \mathbf{0}$. These trajectories account for the forward beam, and constitute the most intense peak of scattering, in agreement with experiments. On the other hand, if the initial \mathbf{P} is *perpendicular* to a set of \mathbf{G}' s of the reciprocal lattice, it is not possible to remove the corresponding first-order term of Eq. (26). In this case the simplified Hamiltonian has a first-order potential to scatter the particle. In two spatial dimensions, the set of directions satisfying $\mathbf{G} \cdot \mathbf{P} = \mathbf{0}$ for a given \mathbf{P} are collinear and the resonant \mathbf{G}' s are parallel, otherwise the following simplification is only an approximation; We further assume the $V_{\mathbf{G}}$ decrease sufficiently fast with $|\mathbf{G}|$, so that we can take the \mathbf{G}_o with the least modulus as the essential *unremovable* term of the potential, which yields

$$\tilde{H} = \frac{1}{2}|\mathbf{P}|^2 + 2\epsilon|V_{\mathbf{G}_o}|\cos(\mathbf{G}_o \cdot \mathbf{x}), \quad (32)$$

a simple pendulum Hamiltonian. The higher-order terms produce crossings of the hyperbolic manifolds of the pendulum Hamiltonian in the usual way^{23,24}. The equation of motion for the \mathbf{P} of the normalized Hamiltonian (32) is

$$\frac{d\mathbf{P}}{dt} = [2\epsilon|V_{\mathbf{G}_o}|\sin(\mathbf{G}_o \cdot \mathbf{x})]\mathbf{G}_o, \quad (33)$$

from which it follows that the momentum kick is

$$\Delta\mathbf{P} = \mathbf{G}_o \int_{-\infty}^{\infty} 2\epsilon|V_{\mathbf{G}_o}|\sin(\mathbf{G}_o \cdot \mathbf{x})dt, \quad (34)$$

a vector parallel to the reciprocal-lattice vector \mathbf{G}_o . An upper bound for the size of the momentum-kick is the maximum momentum excursion along the separatrix^{23,24}

$$|\Delta\mathbf{P}| = |\mathbf{P}_{\max}| = \sqrt{4\epsilon|V_{\mathbf{G}_o}|}, \quad (35)$$

so that we can re-write Eq. (34) in the form

$$\Delta\mathbf{P} \approx \left(\frac{\sqrt{4\epsilon|V_{\mathbf{G}_o}|}}{|\mathbf{G}_o|}\right)\mathbf{G}_o, \quad (36)$$

The interested reader should read the literature^{23,24} on chaotic scattering with a Hamiltonian ODE. The resulting momentum kicks are sensitively dependent on initial conditions as regards magnitude but come in a prescribed direction, i.e., along a vector of the reciprocal lattice. In conclusion; along these resonant initial conditions, the particle suffers stochastic momentum-kicks in the direction of a single reciprocal-lattice vector²⁴ as defined by Eq. (34). This is precisely the von Laue condition²⁵ $\Delta\mathbf{P} = \hbar\mathbf{G}$, in full qualitative agreement with the Bragg-von Laue wavelike scattering of X-rays by crystals²⁵. Our simple model lacks an explicit quantitative size of the angular-momentum kicks, and to calculate the integral

(34) we need the trajectories and the next-order terms that perturb the simple integrable Hamiltonian (32) to a chaotic dynamics. We could adjust $V_{\mathbf{G}_o}$ to obtain an experimental angular-momentum-kick of the mechanism to agree with Eq. (36), i.e., $l_o = \sqrt{4\epsilon|V_{\mathbf{G}_o}|/|\mathbf{G}_o|}$, an adjusting beyond our simplified modeling.

We discussed the above Hamiltonian model as a surprise not often stressed, but even though in qualitative agreement with experiments, modeling with an instantaneous Hamiltonian ODE is hindered *in principle* by the non-interaction theorem²²; The non-interaction theorem²² states that the only two-body motion describable by a Hamiltonian ODE with manifest covariance by the Poincaré group is the free-particle motion²². Essentially, Hamiltonian dynamics is instantaneous, and relativity introduces the finite speed of light, which demands delay-equations of motion with solutions defined *piecewise*, as discussed in appendix A. The no-interaction theorem is not a surprise; delay equations need a history, and only free-moving particles have a straight-line-past-history that can be reconstructed from point-like ODE data. Otherwise, for generic initial data (or boundary data) and nontrivial interactions, we can not expect an ODE to guess an infinite-dimensional history. Since free particles move with constant velocity until a collision, the non-interaction theorem suggests that *if* a Hamiltonian description is of any use, the physical problem at hand must have particles moving with piecewise-constant-velocities, like the scattered charge in our model of Section III.

In sake of a model compatible with the theory of relativity, in the following we discuss scattering by a crystal using neutral differential delay equations and the same model of Section II (essentially a non-Hamiltonian business). Our model places one bound electron at each site of an infinite crystal. The explanation follows in the same way of the double-slit modeling of Section II; Again we assume the incoming charge superimposes a resonant perturbation of period L on the bound orbits at each crystalline site, in the same way explained in Sections II and III. The perturbations are again transferred to the heavy on-site charges to avoid a bowling effect and to heal most of the velocity discontinuities. There remains a small oscillation, so that the out-scattered electron suffers delayed periodic kicks from these synchronized oscillations excited at the crystalline sites. Let \hat{u} be the unit vector along the scattered velocity and $\Delta\hat{u}$ the change of this unitary direction upon scattering. The advanced/retarded delay time $\pm\Delta t_j$ of interaction with the different crystalline sites due to the site-dependent (Δr_j) distances of retardation is²⁵

$$\Delta t_j = \Delta\hat{u} \cdot \Delta r_j, \quad (37)$$

in a unit system where the speed of light is $c = 1$. The favored directions of Bragg scattering are those along which $\Delta t_j = nL$ for an integer n . Using Eq. (37) and the usual properties of reciprocal lattice vectors²⁵ that

$$\mathbf{G} \cdot \Delta r_j = 2\pi n,$$

we find that the favored (resonant) Δu must be along a reciprocal lattice vector \mathbf{G} , i.e.,

$$\Delta u = \frac{L|u|}{2\pi} \mathbf{G}. \quad (38)$$

We see that again a simple Einstein-local microscopic model comes in full qualitative agreement with the Bragg–von Laue wavelike scattering by crystals²⁵. The estimate for the De Broglie length L is the same given in Section III.

-
- * Electronic address: deluca@df.ufscar.br
- ¹ J. A. Wheeler and R. P. Feynman *Rev. Mod. Phys.* **17**, 157 (1945); J. A. Wheeler and R. P. Feynman **21**, 425 (1949).
 - ² A. Bellen and M. Zennaro, *Numerical Methods for Delay Differential Equations* Oxford University Press, NY (2003).
 - ³ J. Hale and S. M. Verduyn Lunel *Introduction to Functional Differential Equations*, Springer-Verlag, New-York (1993).
 - ⁴ O. Diekmann, S.A. van Gils, S.M. Verduyn Lunel and Hans-Otto Walther *Delay Equations*, Springer-Verlag, New York (1995).
 - ⁵ A. Yacobi, M. Heiblum, V. Umansky, H. Shtrikman and D. Mahalu, *Phys. Rev. Lett.* **73** 3149 (1994).
 - ⁶ J. De Luca, *J. Math. Phys.* **50**, 062701 (2009).
 - ⁷ P. A. M. Dirac, *Proceedings of the Royal Society of London, ser. A* **167**, 148 (1938).
 - ⁸ K. Hess and W. Philipp, *Foundations of Physics* **35** 1749 (2005).
 - ⁹ A. P. Jauho, K. M. Pichungin and A. Sadreev *Phys. Rev. B* **60**, 8191 (1999).
 - ¹⁰ A. Tonomura, J. Endo, T. Matsuda and T. Kawasaki, *Am. J. Phys.* **57**, 117 (1989).
 - ¹¹ C. Jonnson, *Zeitschrift fur Physik* **42** 4 (1961).
 - ¹² R.P. Feynman, R. B. Leighton and M. Sands, *The Feynman Lectures on Physics– Quantum Mechanics*, Addison-Wesley Publishing, Reading (1963).
 - ¹³ P. Rodgers, *Science’s 10 most beautiful experiments*, *New York Times* (September 2002).
 - ¹⁴ J.D. Jackson, *Classical Electrodynamics* Second Edition, John Wiley and Sons, New York (1975).
 - ¹⁵ J. De Luca, *Physical Review E* **82** 026212 (2010).
 - ¹⁶ J. De Luca, *Physical Review E* **73** 026221 (2006).
 - ¹⁷ J. W. M. Bush, *Proc. Natl. Acad. Sci USA* **107**; 17455 (2010) and Fort E, Eddl A, Boudaoud A, Moukhtar J, Couder Y, *Proc. Natl. Acad. Sci USA* **107**, 17515 (2010).
 - ¹⁸ C. Davisson and L. H. Germer, *Nature* **119**, 558 (1927).
 - ¹⁹ A. Zeilinger, R. Gahler, C. G. Shull, W. Treimer and W. Mampe *Reviews of Modern Physics* **60**, 1067 (1988).
 - ²⁰ W. Duane, *PNAS* **9**, 158 (1923).
 - ²¹ A. Compton, *PNAS* **9**, 359 (1923).
 - ²² D. G. Currie, T. F. Jordan and E. C. G. Sudarshan, *Rev. Mod. Phys.* **35**, 350 (1963), G. Marmo, G.N. Mukunda and E. C. G. Sudarshan, *Phys. Rev. D* **30**, 2110 (1984) and also in "The theory of Action-at-a-distance in Relativistic Particle Dynamics", Edited by E. H. Kerner, Gordon and Breach Publishers, New York (1972).
 - ²³ B. V. Chirikov, *A universal instability of many-dimensional oscillator systems*, *Physics Reports* **52**, 265 (1979).
 - ²⁴ A.J. Lichtenberg and M.A. Lieberman, *Regular and Chaotic Dynamics* Second Edition, Springer-Verlag, New York (1992), pgs. 25-29
 - ²⁵ N. W. Aschcroft and N. D. Mermin, *Solid State Physics* Holt, Rinehart and Winston, New York (1979).
 - ²⁶ J. Mehra, "The beat of a different drum" (*the life and science of Richard Feynman*) Claredon Press-Oxford (1994). (chapter 5)
 - ²⁷ J. De Luca, *Physical Review Letters* **80**, 680 (1998), *Physical Review E* **58**, 5727 (1998), *Physical Review E* **62**, 2060 (2000), V. Mehra and J. De Luca, *Physical Review E* **61**, 1199 (2000) and *Physical Review E* **64**, 085306 (2001).
 - ²⁸ J. N. Dodd, *European Journal of Physics* **4**, 205 (1983).
 - ²⁹ C. T.H. Baker and C. A. H. Paul *Applied Numerical Mathematics* **56**, 284 (2006).